JMEPEG (2012) 21:575–584
DOI: 10.1007/s11665-012-0184-5

1059-9495/$19.00

Anisotropy of Wetting and Spreading in Binary Cu-Pb Metallic System: Experimental Facts and MD Modeling

Vadim Timoshenko, Vladimir Bochenkov, Vladimir Traskine, and Pavel Protsenko

(Submitted October 31, 2011; in revised form February 2, 2012)

Contact angle for millimeter-size drops of lead on {100} and {110} surfaces of monocrystalline copper and on polycrystalline copper was determined by means of dispensed drop technique at 450 °C under He-H_2 atmosphere. It was demonstrated that the wetting anisotropy (a difference between contact angles on differently oriented substrates) is not exceed a few degrees. Spreading kinetics was found to be different for the first and second drops deposited on each substrate. This result was interpreted as an effect of a lead precursor film formation on the substrate surface. Molecular dynamics simulations of the lead drop spreading over {111}, {100}, and {110} surfaces of monocrystalline copper confirm the weak anisotropy of equilibrium contact angle and a formation of lead precursor film on copper surface in front of wetting line.

Keywords anisotropy, contact angle, copper, lead, spreading

1. Introduction

Interfacial reactivity is known to be strongly influenced by the crystallographic orientation of a solid surface. This is widely used in electronics to produce silicon-based microelectromechanical devices (MEMS). At the same time the effect of anisotropic wetting (observation of different equilibrium contact angle of liquid B on different crystallographic planes of substrate A) is far from been clearly understood. A simple idea is lying under the concept of wetting anisotropy: consider a liquid drop forming an equilibrium contact angle on the surface of a flat insoluble crystalline substrate being in an equilibrium with vapor phase. Than the equilibrium contact angle θ^{hkl} is linked to the interfacial energies of solid-gas, solid-liquid, and liquid-gas (σ_{sg}^{hkl}, σ_{sl}^{hkl}, and σ_{lg}) boundaries through the classical Young-Dupré equation:

$$\cos\left(\theta^{hkl}\right) = \frac{\sigma_{sg}^{hkl} - \sigma_{sl}^{hkl}}{\sigma_{lg}}. \quad \text{(Eq 1)}$$

If the difference between the solid-gas and solid-liquid interfacial energies depend on the substrate plane orientation {hkl}, than the anisotropy of contact angle should be observed.

Let us restrict our consideration to binary liquid metal/solid metal (or semiconductor) systems. Despite of a substantial number of experimental results, reviewed by Povstenko (Ref 1) and recently by Chatain (Ref 2), the relationship between the structure of the solid surface and contact angle is not clearly demonstrated. Available experimental data on contact angle anisotropy could be divided into two parts: wetting by "macroscopic", i.e., millimeter-size droplets and wetting by micron-size drops formed from PVD-produced films.

Experiments of the first type on In/Ge system were reported by Vyatkin (Ref 3, 4). Contact angle anisotropy was studied by a sessile drop technique in vacuum (7×10^{-5} Pa): a peace of low-melting metal was heated on a monocrystalline substrate. At 200 °C contact angle was found to be equal to 160°, which is an indication of a presence of an oxide film on the substrate surface (and probably on the surface of liquid drop). At 550 °C the noticeably different contact angles equal to 60°, 75°, and 85° were observed on the {111}, {110}, and {100} surfaces correspondingly. Here a significant solubility of Ge in liquid In (about 12 at.% at 550 °C (Ref 5)) should be underlined. Moreover, a significant dependence of contact angle on heating rate was observed: at 550 °C for the heating rate of 100-150 deg/h the contact angle θ was equal to 60° for In/Ge{111} and θ ≈ 75° for In/Ge{110}, whereas for the higher heating rate of 100-150 deg/min the contact angle close to 80° was observed for In/Ge{111} system. Grigorenko (Ref 6) has observed similar tendency for the contact angle of (In-Sn-Ge) alloy on Ge surface: at 500 °C in high vacuum (1.33×10^{-3} Pa) θ = 54° was observed on {111} surface and 74° on {100} surface. An alloy was melted separately in a graphite crucible and dropped down onto the substrate through an orifice in the bottom of the crucible. This technique did not allow the formation of a liquid drop saturated with Ge, because In-Sn eutectic point is low and Ge solubility depends significantly on the temperature.

Experiments of the second type are based on the deposition of low-melting metal by PVD on a substrate followed by heating over the fusion temperature and formation of the micron-size droplets as a result of de-wetting process. Wettability of Si by micron-size Au drops formed from PVD film was

This article is an invited submission to JMEP selected from presentations at the Symposia "Wetting, soldering and brazing" and "Diffusion bonding and characterization" belonging to the Topic "Joining" at the European Congress and Exhibition on Advanced Materials and Processes (EUROMAT 2011), held September 12-15, 2011, in Montpellier, France, and has been expanded from the original presentation.

Vadim Timoshenko, Vladimir Bochenkov, Vladimir Traskine and **Pavel Protsenko,** Chemistry Department, Lomonosov Moscow State University, Leninskie Gory, 1-3, Moscow, Russia. Contact e-mail: protsenko@colloid.chem.msu.ru.

studied by Ressel et al. (Ref 7). A significant difference between the contact angles on {100} and {111} surfaces was observed. At $T = 650$ °C the contact angle is equal to 43° on {111} surface and 20° on {100} surface. The same technique was used by Wynblatt et al. to study the anisotropy of contact angle for solid droplets in Pb/Al (Ref 8, 9) and Pb/Cu (Ref 10) systems. Experiments were performed in UHV with preliminary cleaning of the surface by ion sputtering. A significant anisotropy was observed, though the effect of surface orientation was opposite: $\theta = 27.3°$ was measured for Pb/Al{111} system, $\theta = 41.1°$ for Pb/Al{100}, $\theta = 48.3°$ for Pb/Cu{111}, and $\theta = 34°$ for Pb/Cu{100}.

A brief overview of literature data demonstrates that the study of wetting anisotropy in metallic systems at elevated temperature is a particularly difficult task. The most important difficulties are:

1. The presence of oxide layers on substrate and liquid drop surfaces. In the absence of oxide films a good wetting ($\theta < 90°$) should be observed for any metal/metal couple including practically immiscible systems such as Pb/W (Ref 11, 12). Different crystallographic planes are also known to have different affinity to impurities in the gas phase (mainly to oxygen) which could provoke wetting anisotropy due to selective decrease of substrate energy.
2. The dissolution of a substrate during spreading is known to change significantly the observable contact angle (Ref 13) because the solid-liquid interface is not macroscopically flat. Anisotropic spreading could be confused with anisotropic dissolution in this case. For In/Ge and Au/Si systems the effect of dissolution on contact angle should not be ignored.

The present study was motivated by the lack of the reliable data on contact angle anisotropy in metallic systems. Liquid Pb/solid Cu couple was selected due to the several reasons: (i) absence of intermetallics and low mutual solubility; (ii) comparatively low affinity of both metals to oxygen, allowing to remove the oxide films from the surfaces without ion sputtering; (iii) presence of reliable literature data on the anisotropy of solid Cu surface energy and Pb-Cu interfacial energy. In order to analyze the details of spreading process on an atomic scale, a molecular dynamic simulation of Pb/Cu system was performed in parallel to the experiment.

2. Experimental

The experimental setup used for studying wetting and spreading of molten lead on copper surface is presented in Fig. 1. It consists of the vacuum oven equipped with the samples support (5), melt dispensing system (4), and optical system.

Vacuum oven consists of oil-diffusion pump-based vacuum system and a heating volume. A set of tungsten strips form the cage-type resistive heating element (3). The heater is surrounded by molybdenum radiation insulation screens (2) and fixed in water coolant housing (1) of the oven. The oven allows carrying experiments in temperature range of 300-1400 °C in vacuum down to 5×10^{-6} mbar or in reducing atmosphere of He-5%H_2 gas mixture up to the atmospheric pressure.

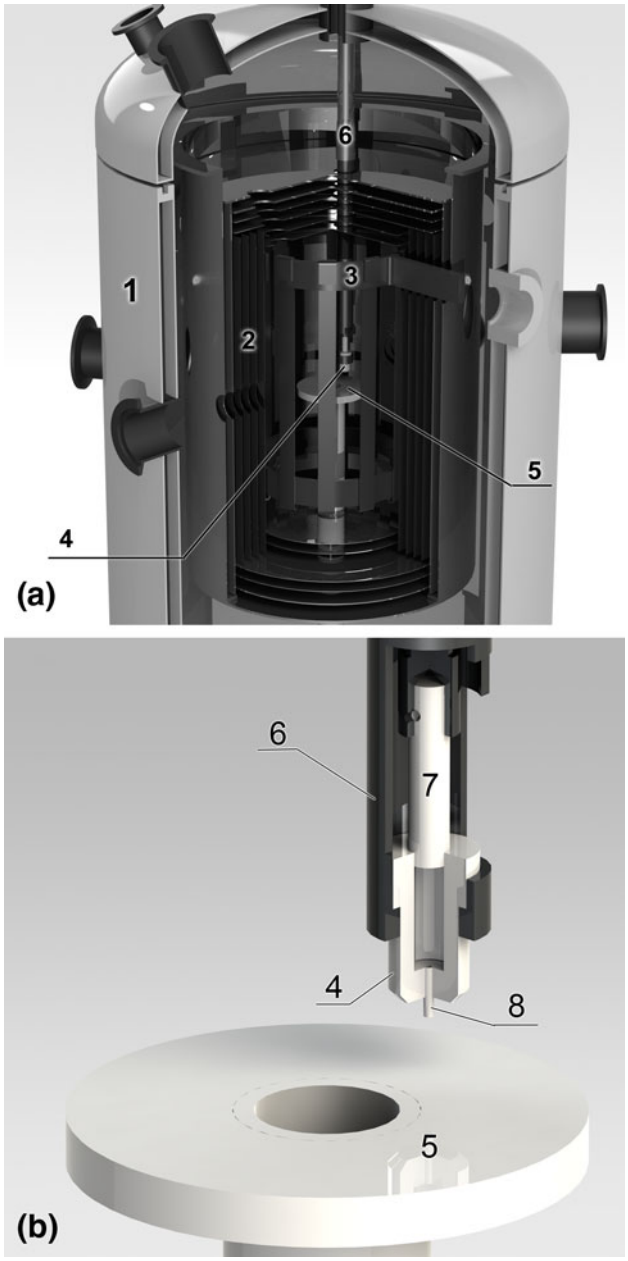

Fig. 1 (a) Experimental setup designed for studying wetting by dispensed drop technique at high temperature in controlled atmosphere. 1—Vacuum chamber with water-cooled stainless steel housing, 2—molybdenum radiation shields, 3—tungsten resistance heater, 4—alumina dispenser, 5—alumina substrate support, 6—dispenser manipulation system. (b) Alumina dispenser. 7—alumina plunger, 8—alumina capillary

The melt dispensing system (Fig. 1b) consists of an alumina crucible with plunger (7) and a capillary tip (8). The crucible is inserted in a specially designed holder (6). It allows moving the plunger inside the crucible to extrude the drop of melt. There is another mechanism to adjust position of dispenser as a whole up and down. Dispensing system is made of stainless steel and molybdenum and can work at temperatures up to 1400 °C in vacuum or reducing atmosphere. A water circulation is used to cool the dispensing system.

Dispensed drop technique has several advantages comparing to classical sessile drop technique: (i) it is possible to remove

the oxide films from the surface of the liquid by extrusion of the drop through the thin capillary; (ii) a liquid can be equilibrated with the high melting point components directly inside the crucible before the contact with substrate; (iii) the substrate can be subjected to heat treatment at high temperature separately from the low melting point sample. This technique is successfully exploited by several research groups to study wettability at elevated temperatures (Ref 11).

The sample support is the alumina rotatable table (5) situated in the center of the heating zone which is fixed at the bottom of the shields. This allows us to place a number of samples on the table and investigate several drops in a single experiment.

The optical system is based on the rapid video camera "FastVideo-400". Backlight illumination is carried out by high intensity discharge lamp with collimator system that produces a convergent high intensity light beam. It is necessary to produce an acceptable light flux to fulfill the camera sensitivity at the shutter time of several microseconds. This system allows us to acquire sharp images of spreading drop at rates up to 1000 frames/s with an acceptable resolution.

The polycrystalline copper of 99.999% purity was used without any additional purification. Copper monocrystal was obtained from Institute of Solid State Physics RAS. The samples were cut by electrosparking cutting machine to produce 2 mm thick slides. The shape of copper samples was the following: 10×2 mm polycrystalline disks, $10 \times 10 \times 2$ mm {100} monocrystals, and $10 \times 12 \times 2$ mm {110} monocrystals. Copper slides were ground using SiC-paper and then polished with diamond pastes to 1 μm. The samples are rinsed by dilute HCl and water to eliminate oxide layers and then ultrasonically cleaned with acetone-ethyl alcohol mixture and dried by pressurized air immediately before placed into vacuum chamber.

To form the melt we used lead granules of 99.9999 % purity. The lead and calculated amount of copper needed to form saturated solution of copper in lead at experiment temperature were placed in alumina crucible with plunger.

The following experimental procedure was used to compare wettability of copper substrates with different surface orientation. Three samples of Cu-polycrystal, {100}, and {110} monocrystals were placed on the alumina support inside the furnace, than the installation was evacuated down to 5×10^{-6} mbar total pressure and heated up to 450 °C. At this moment He-H_2 gas mixture was introduced to 0.5 bar total pressure. The furnace was heated up to 560 °C, the temperature was maintained for 20 min and then the installation was cooled down to 450 °C. The first Pb drop was deposited on polycrystalline Cu substrate and drop shape evaluation during spreading was registered. The final base diameter of the drop varies from 2.5 to 4.5 mm. After that the thermal treatment at 560 °C was repeated. Than the sample support was slightly rotated to shift the substrate by a few millimeters and the second drop was deposited on the same substrate without interference with substrate edges and without coalescence with the first drop (Fig. 2). The procedure of two drops deposition was repeated for the {100} and {110} monocrystalline substrates.

The drop shape parameters (contact angle and drop base diameter) were extracted from the sequence of spreading drop images (Fig. 3). On the initial stage of spreading, when the drop shape was significantly perturbed, contact angles were measured by tangent method. For the sessile drops that

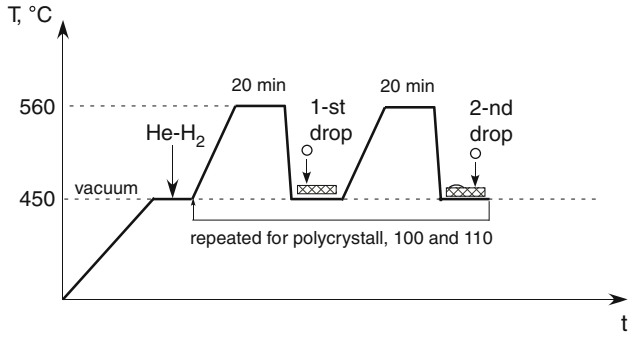

Fig. 2 Experimental procedure explored to deposit consequently two drops on the surface of three substrates

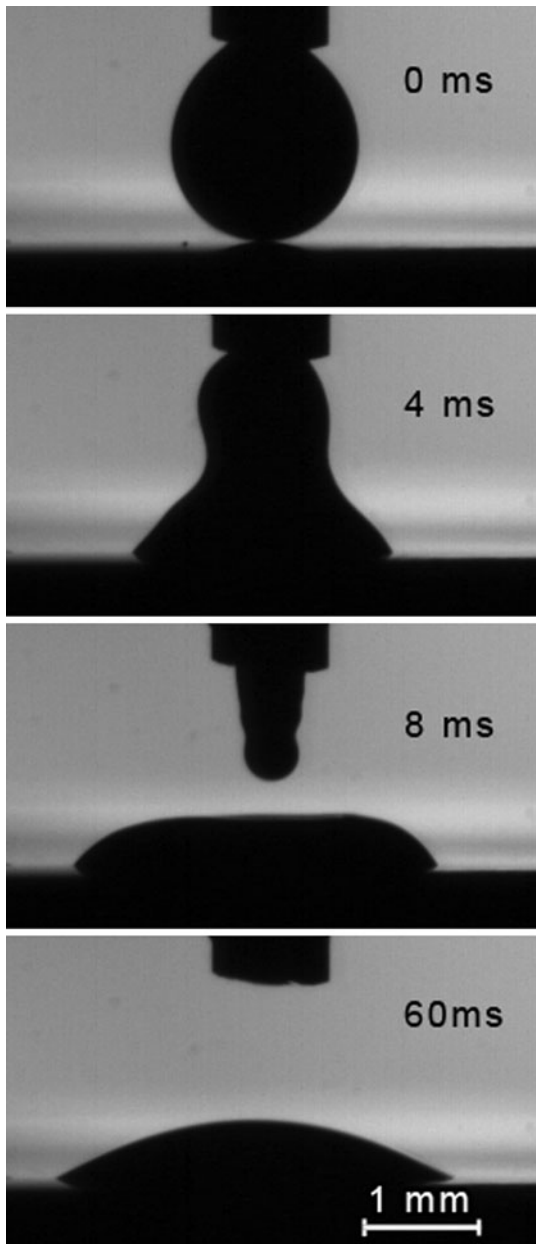

Fig. 3 Deposition and spreading of the Pb-Cu drop on the {110} Cu surface at 450 °C in He-H_2 atmosphere

achieved the capillary equilibrium, both tangent and Laplace equation fitting methods were used. The precision of the contact angle measurements was ±1°.

3. Modeling

The simulations of spreading of the liquid Pb over solid Cu{100}, Cu{110}, and Cu{111} surfaces have been carried out using classical molecular dynamics (MD). The calculations have been run on a SKIF-MSU supercomputer using efficient parallel Large-scale Atomic/Molecular Massively Parallel Simulator (LAMMPS) (Ref 14).

Undoubtedly, the choice of the right interatomic potential that can accurately describe the potential energy surface in binary Pb-Cu system and thus reproduce the experimental bulk phase diagram, is of primary importance for obtaining the reliable results. As well as for the other metallic systems, the multibody contribution to the potential energy of each atom is large enough to be explicitly taken into account, as in the embedded atom method (EAM) formalism (Ref 15). In the present work we used the EAM interatomic potential for Pb-Cu system (Ref 16) based on the previously derived potentials for pure Pb (Ref 17) and Cu (Ref 18) and fitted to reproduce well the experimental values of liquid alloy heat of mixing and the binary phase diagram. It has been used previously to study the wetting phenomena (Ref 19-22) and thus was chosen to be used in the present work.

The initial state of a system was constructed by a Cu surface and Pb spherical droplet placed in contact with each other at 327 °C. The Cu crystal surface was created with either (100), (110), or (111) face oriented towards z direction. Periodic boundary conditions have been applied in x and y dimensions, thus forming two free crystal surfaces. The lateral size of a simulation cell has been selected large enough to allow Pb spreading without covering the whole Cu surface, namely 115×115 nm. The lowest layer of atoms was kept fixed, whereas the other atoms were allowed to relax. The total thickness of the Cu slab is four atomic layers (0.7 nm). Depending on the orientation, the Cu substrate contained approximately from 500,000 to 800,000 atoms. The Pb droplet was represented as a sphere of 16 nm in diameter, containing 72,484 atoms. The liquid Pb has been equilibrated at constant temperature prior to contacting the Cu surface. The temperature in the system has been kept constant using the Langevin thermostat, time integration was done in *NVE* ensemble with the time step of 5 fs. Typical MD trajectory length was 40 ns. The simulation of 10 ns required approximately 17 h on 256 cores of a supercomputer.

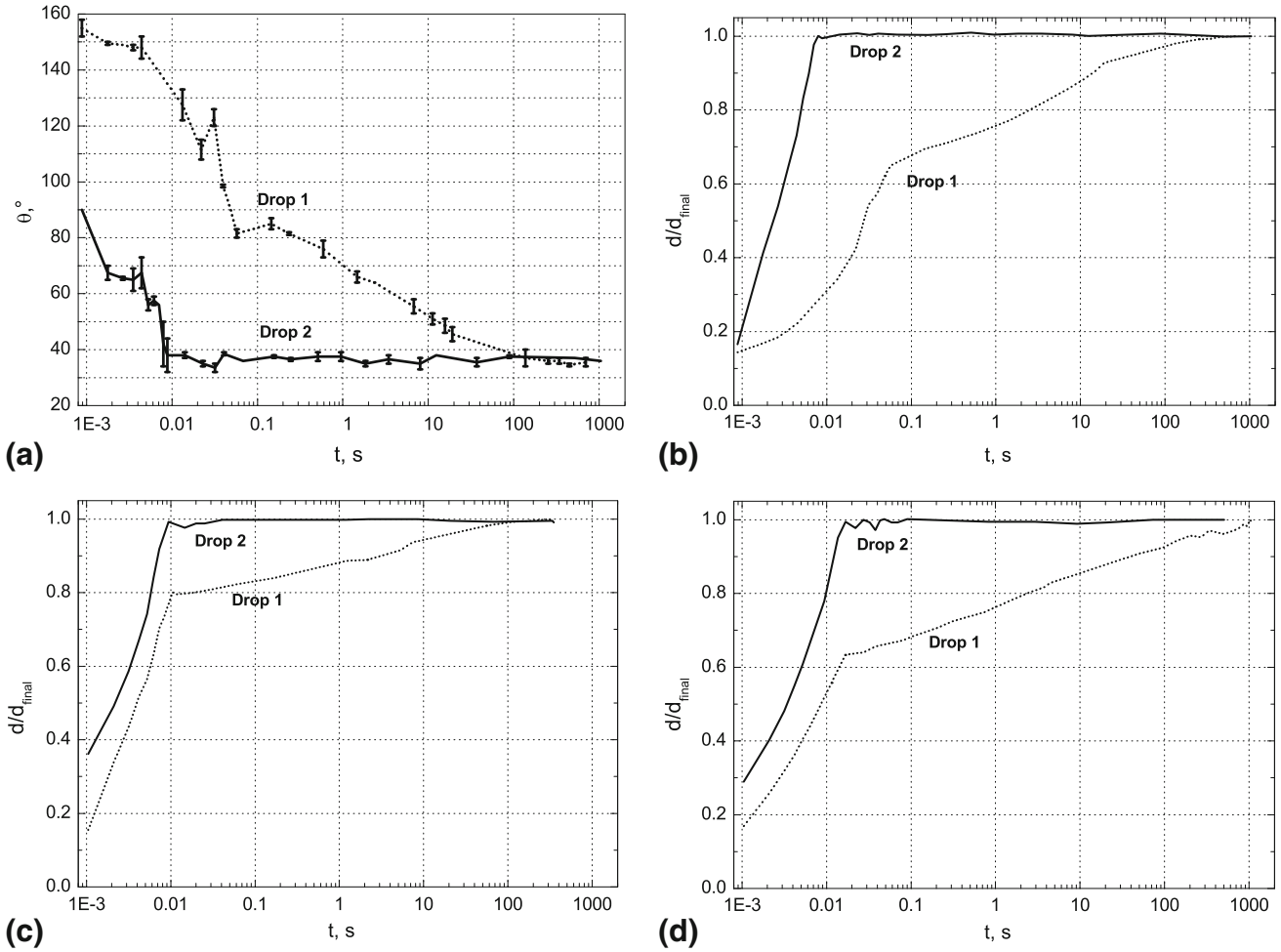

Fig. 4 Contact angle and relative drop base diameter vs. time for the first and second droplet of Pb-Cu alloy deposited on the Cu{100} (a, b), Cu{110} (c), and polycrystalline Cu (d) surfaces at 450 °C in He-H_2

The contact angles were extracted from the simulation snapshots by construction of the Pb density profiles in two mutually orthogonal directions. More specifically, to construct the density profile in *x*-*z* projection the number of Pb atoms was counted for every volume $(x_i;x_i + \Delta x] \times [y_1;y_N] \times (z_k;z_k + \Delta z]$, where $i = 1, \ldots, N$, $j = 1, \ldots, M$ and the drop is completely inside the volume $(x_1;x_N) \times (y_1;y_N) \times (z_1;z_M)$. Then two edges of the drop have been determined for every z_k, $1 \le k \le M$. The same procedure was repeated for the *y*-*z* projection. After that the two contact angle values have been determined from every projection, which resulted in four values that were averaged.

4. Results

4.1 Dispensed Drop Experiments

The dependencies of the contact angle on the spreading time for Pb-Cu/Cu{100} system and the relative drop base diameter on the spreading time for Pb-Cu melt on Cu{100}, Cu{110}, and polycrystalline Cu are presented in Fig. 4. A pronounced difference in spreading behavior for the first and the second drop was observed. The first drop demonstrates relatively complex spreading behavior. During the initial fast stage of spreading (0-50 ms) the contact angle decreases down to 80°. Such a high value could be an indication of a copper surface pollution. Than the contact angle gradually decrease during ~100 s to 35°. It should be noticed that the time of the slow stage varied from 10^2 to 10^3 s and the final contact angle is scattered in the range of 35°-45°.

The second drop demonstrates completely different behavior. Equilibrium contact angle equal to 35° was observed within ~10 ms—typical time needed for millimeter-size droplet to reach equilibrium in non-reactive system (Ref 11).

The effect of substrate orientation on the contact angle did not exceed a few degrees. The time dependencies of contact angle and drop base diameter for the second drops on Cu{100} and Cu{110} substrates are presented in Fig. 5. It can be seen from presented data that equilibrium contact angle and final base diameter is reached after ~10 ms on both substrates. Contact angle for Pb-Cu drop on polycrystalline copper is close to the one obtained on monocrystalline substrates. Average values obtained from three independent experiments are presented in Table 1.

After the solidification, the Cu substrates with Pb drops were examined with optical microscopy. Dewetting zones were not observed on substrate surface. Spreading anisotropy was not detected on {100} monocrystalline and on polycrystalline substrates. In the case of {110} monocrystals, a different behavior was observed for first and second deposited drops. Triple line formed by the first drops had elliptical shape, axis ratio of ellipses ranged from 1.1 to 1.3 with long axis parallel to ⟨110⟩ direction of substrate. Second drops forms circular triple line, axis ratio was well under 10% (Fig. 6).

4.2 MD Simulation

The consequent images of Pb drops spreading over (100), (111), and (110) Cu monocrystals are presented in Fig. 7, 8, and 9. Only Pb atoms are presented in the figures for clarity. The dependence of drop base diameter and precursor film diameter on time is presented for (100) surface in Fig. 10. The simulation results demonstrate that on the first stage of spreading (from θ = 180° at $t = 0$ to θ close to 40°) the drops spread as a whole over all substrates during 3-4 ns. The following sharp decrease of the triple line velocity is coupled with the formation of the precursor film. The precursor film is one-monolayer thick on the (110) surface and two-monolayer thick on the (111) and (100). On the second stage of spreading the precursor film continues to extend over Cu surface leaving behind the triple line. The triple line velocity approaches zero at ~10 ns and the final contact angle value close to 30° (for all considered surfaces) is reached at the same moment (Table 1). The last spreading stage (10-20 ns) is characterized by the

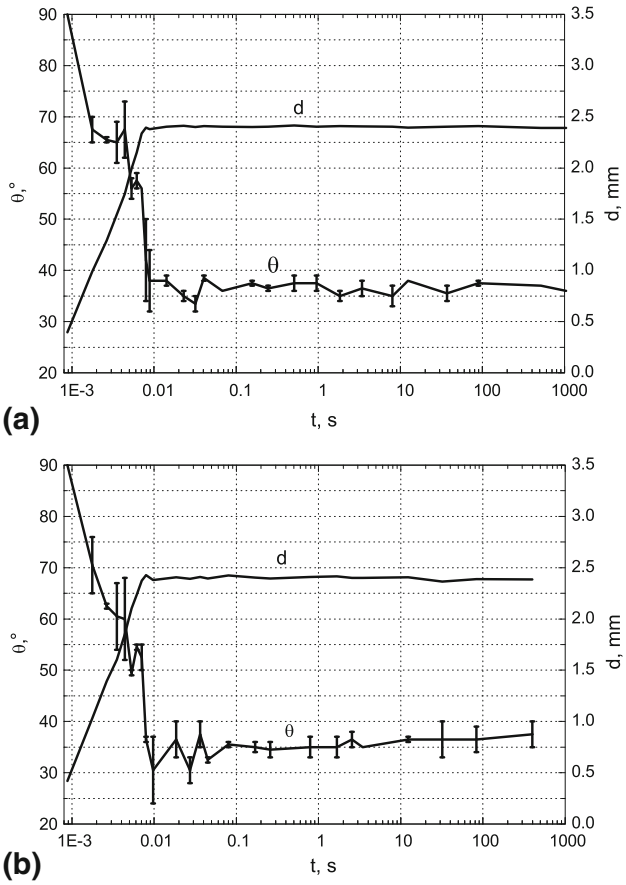

Fig. 5 Contact angle and drop base diameter vs. time for Pb-Cu alloy deposited on the Cu{100} (a) and Cu{110} (b) surface (second drops)

Table 1 Values of equilibrium contact angle of Pb drop on Cu substrates with different surface structure

	Dispensed drop (this work)	MD simulation (this work)	Solid state wetting(a) (Ref 10)
T, °C	450	327	310
{111}	…	32°	48.3° ± 1.75°
{100}	36° ± 3°	31°	34.0° ± 1.57°
{110}	32° ± 4°	31°	…
Polycrystal	32° ± 2°	…	31.8° ± 3.75°

(a) Standard deviation of measured contact angle is taken as error

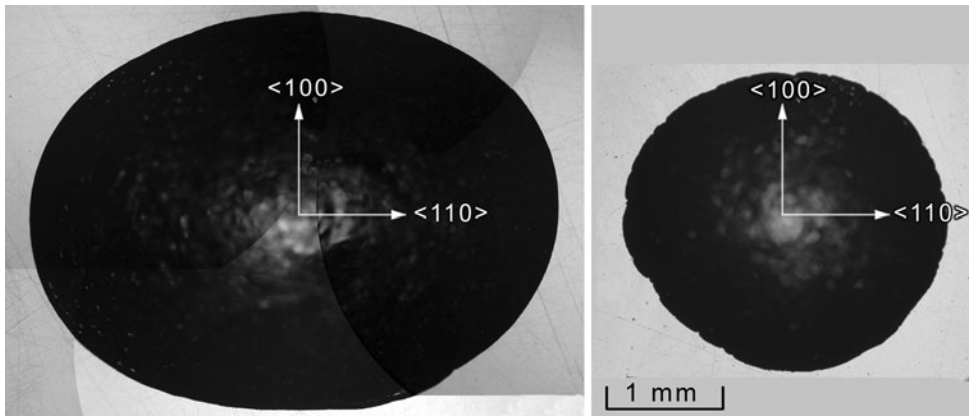

Fig. 6 Top view of solidified first (a) and second (b) Pb drops deposited on {110} Cu surface (optical micrograph). Orientation of copper substrate is marked on the top of the drops

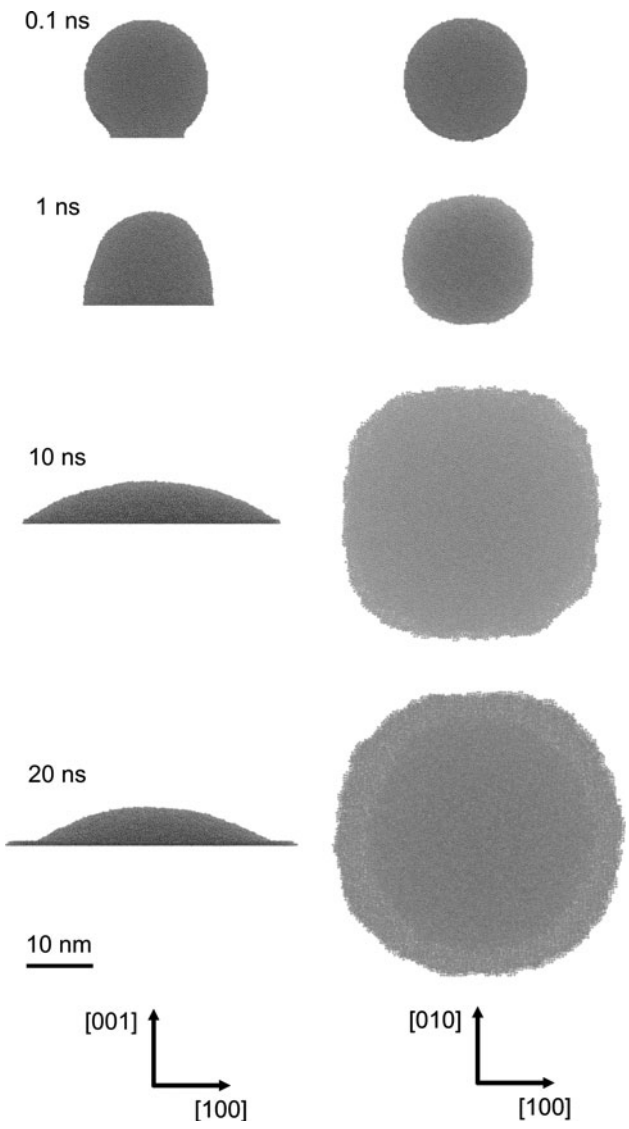

Fig. 7 Consequence of Pb drop snapshots on (100) Cu surface from MD simulation, side view is presented in the left column and top view in the right column. Orientation of the copper substrate is marked in the bottom

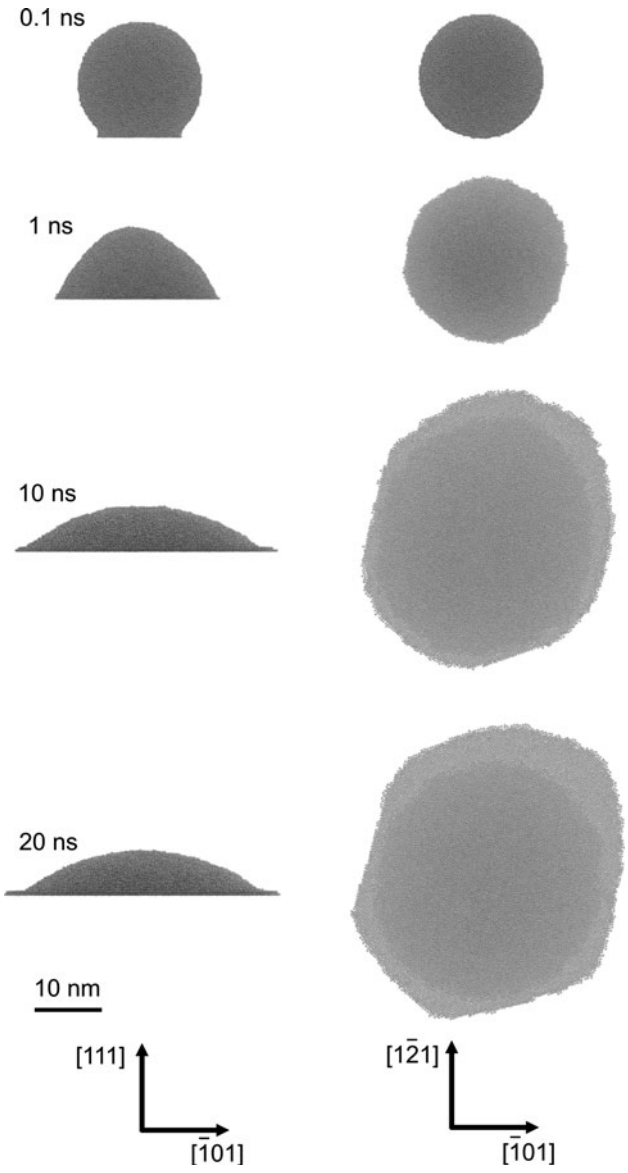

Fig. 8 Consequence of Pb drop snapshots on (111) Cu surface from MD simulation, side view is presented in the left column and top view in the right column. Orientation of the copper substrate is marked in the bottom

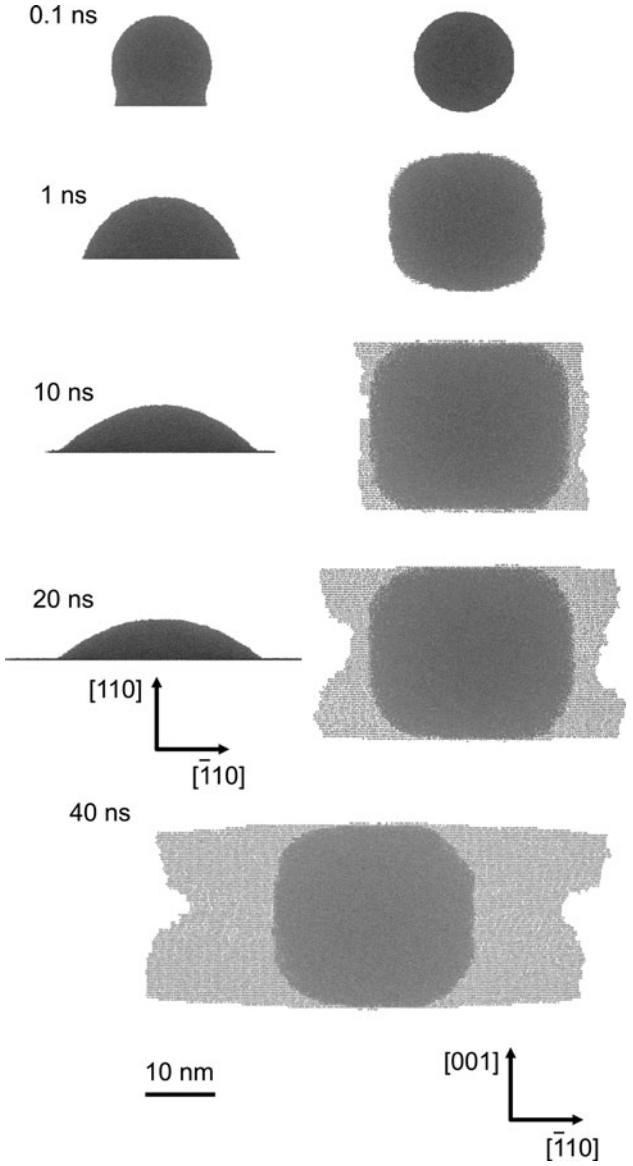

Fig. 9 Consequence of Pb drop snapshots on (110) Cu surface from MD simulation, side view is presented in the left column and top view in the right column. Orientation of the copper substrate is marked in the bottom

immobile triple line and growing precursor film. The dependencies of the contact angle and drop base diameter on time in logarithmic scale are presented in Fig. 11.

The top view of the fragments of precursor film on (100), (111), and (110) surfaces are presented in Fig. 12. The films on (111) and (110) surfaces are of crystalline nature, whereas the film on the (100) surface is more disordered. In all cases the structure of the precursor film is determined by the structure of underlying copper surface: two hexagonal close-packed layers on (111), two square packed layers on (100), and one rectangular packed layer on (110). The interatomic distances in all cases are smaller comparing to ones in bulk Pb. The density of Pb atoms in the film corresponds to 2.18 monolayers for (111) (a monolayer of Pb atoms on the same surface of Pb is taken as reference), 2.35 for (100), and 1.55 for (110).

The substrate orientation essentially affects the shape of the precursor film and the drop symmetry (Fig. 7, 8, and 9). The

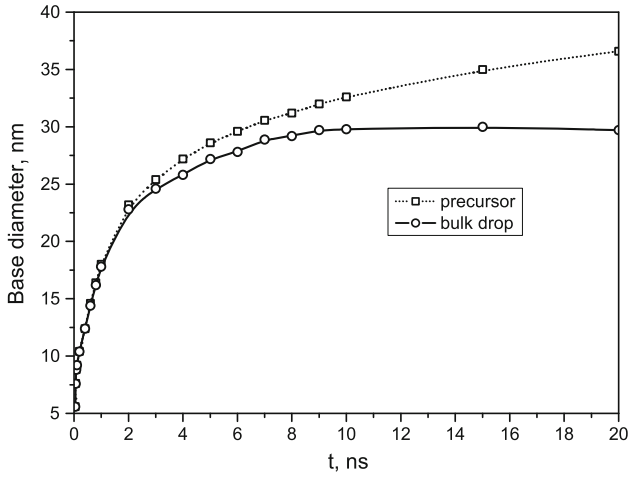

Fig. 10 Drop base diameter and precursor film diameter vs. time for Pb drop on (100) Cu surface (MD simulation)

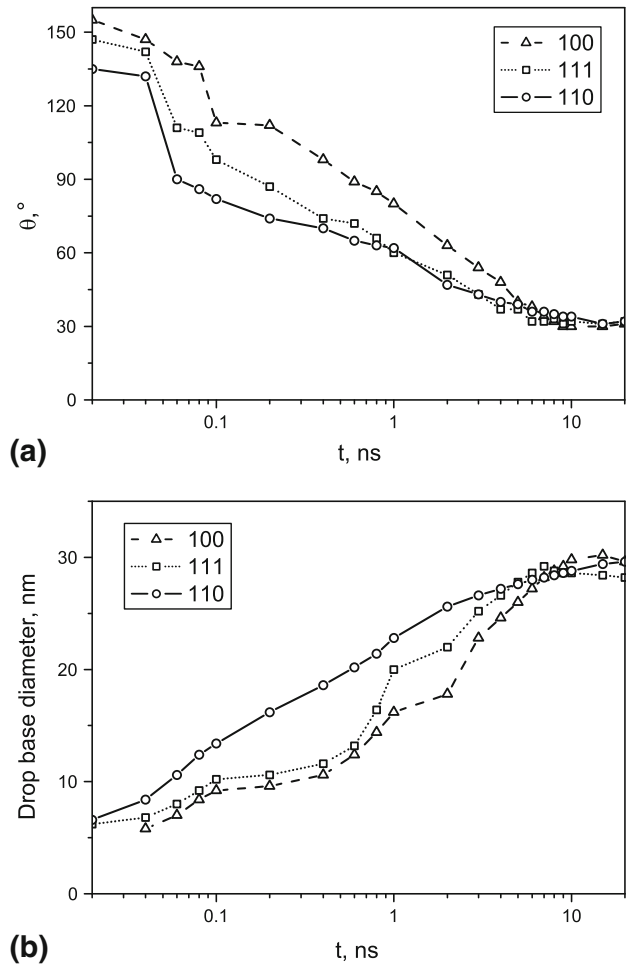

Fig. 11 Contact angle (a) and drop base diameter (b) vs. time for Pb drop spreading over monocrystalline Cu substrates (MD simulation)

most disordered film on (100) surface demonstrates tendency to form rounded square shape (at 10 ns), but almost circular shape was observed on the last stage of spreading (20 ns). The bulk drop does not deviate significantly from the spherical cap shape.

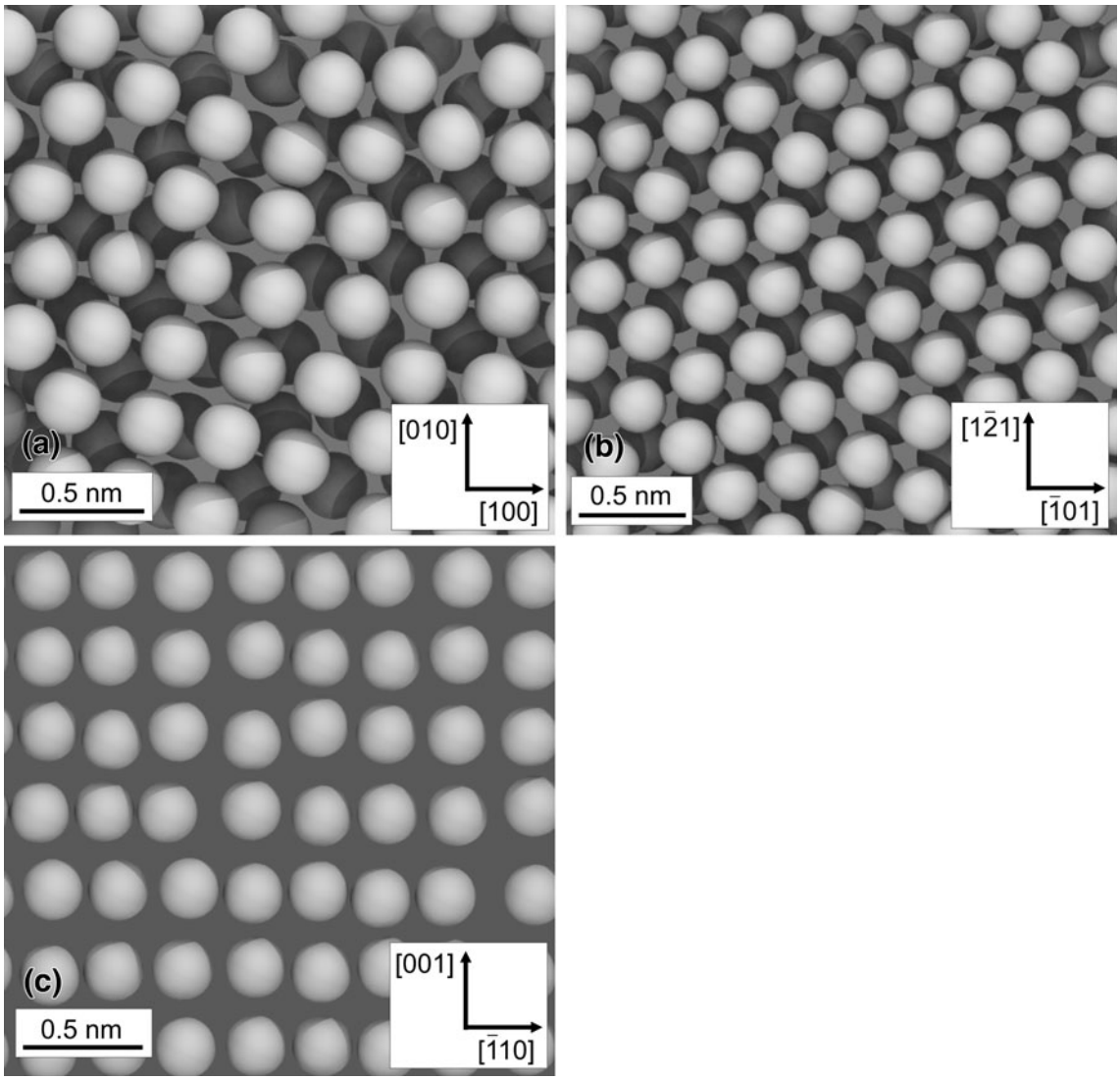

Fig. 12 Structure of Pb precursor films on (100) (a), (111) (b), and (110) (c) Cu surface (MD simulation)

The precursor film on (111) surface becomes hexagonal-shaped on the last stage of spreading. This is in agreement with the crystalline character of precursor. In the same time, the triple line of bulk drop on (111) surface is circular. Spreading of precursor over (110) surface is strongly anisotropic. The precursor do not spreads ahead triple line in [001] direction and intensively spreads in [$\bar{1}$10] direction. The film has specific shape with depression in [$\bar{1}$10] direction opposite to the drop center. The bulk drop shape evaluates from spherical cap on the initial step of spreading (before precursor formation) to the rounded rectangular at intermediate step. During the last step of spreading drop demonstrates tendency to round triple line. In the case of (110) substrate time needed for complete the equilibration of bulk Pb drop on the top of precursor film, seems to be higher than 20 ns. Thus the equilibrium contact angle, estimated from MD simulation, should be several degrees less than 30°.

5. Discussion

Dispensed drop technique was used for the first time to study wettability in Pb-Cu/Cu system. It gives us an advantage to study in details the first stage of spreading. A significant difference in behavior of the first and second drops, observed on both monocrystalline and polycrystalline substrates could be explained by formation of lead precursor film after first drop deposition. The formation of such film, first suggested by Bailey (Ref 23) to explain reduction of solid Cu surface tension in the presence of Pb vapor, was observed directly by scanning Auger microprobe (Ref 10) and Rutherford backscattering (Ref 24). All the experiments presented in this work were performed under He-H_2 atmosphere with moderate preliminary heat treatment at 560 °C for 20 min. Thus, the Pb deposition on Cu surface through the vapor phase before drop transfer is unlikely. We suppose that spreading kinetics for first drop is linked to displacement of adsorbed on Cu surface species (hydrogen, carbon, other impurities from gas phase) by Pb atoms. As the amount of impurities can vary from sample to sample, spreading time for the first drop was systematically not reproducible. Quantitative interpretation of spreading kinetics is difficult in this case. Improvement of experimental procedure (purification of furnace atmosphere and copper surface) is needed to perform this analysis.

When the substrate with already deposited Pb drop heated again up to 560 °C for 20 min mobility of precursor film

increases and it is able to cover all available surface of Cu substrate and to replace the surface impurities. Thus, the second drop is deposited directly on Pb precursor film and spreads without kinetic limitations on triple line within ~10 ms similar to many non-reactive liquid metal/solid metal couples, such as Pb/Fe (Ref 11) and Pb/W (Ref 12). It is suggested in Ref 11 that inertial forces predominantly controls spreading in this case. Due to complex liquid shape evolution (Fig. 3) and flow behavior inside the drop analytical model of such spreading did not suggested to the moment.

A proposed interpretation for the spreading difference of "first drop" and "second drop" is supported by the observation of spreading anisotropy for the first drop on {110} surface. According to MD simulation spreading of the precursor film toward ⟨001⟩ direction is considerably slower than toward ⟨110⟩ direction, leading to the noticeable elongation of the precursor film in ⟨110⟩ direction. The second drop, deposited on the precursor film, should be axisymmetric, because the impediments for circular triple line formation are vanished. The formation of axisymmetric second drop on {110} surface is confirmed experimentally (Fig. 6).

Both experimental and simulation results indicates that the contact angle anisotropy is negligible in Pb/Cu system (Table 1). To understand this result the anisotropy of solid-vapor and solid-liquid interfacial energies should be considered. The surface energy of solid copper in the absence of Pb vapor is known to be almost isotropic. This fact was recently confirmed by the study of equilibrium shape of copper monocrystals on sapphire support (Ref 25). It was shown that at 1240 K $\sigma_{sg}\{110\}/\sigma_{sg}\{100\} = 1.012$ and $\sigma_{sg}\{100\}/\sigma_{sg}\{111\} = 1.004$. We do not have any data on copper surface energy anisotropy at low temperature (which could be potentially higher than one close to copper fusion point), but there is an indirect evidence, that even at Pb fusion temperature solid copper surface energy is isotropic. The direct measurements of Pb adsorption on solid Cu by AES shows, that Pb atoms density is similar on both {111} and {100} surfaces and equal to 0.7-0.8 monolayers in equilibrium with solid Pb drops at 310 °C (Ref 10). As the adsorption of Pb is similar for different Cu substrate orientation, the decrease of solid Cu surface energy in equilibrium with Pb should be the same.

The anisotropy of solid-liquid interfacial energy in Pb-Cu system was recently studied by Felberbaum (Ref 26). The equilibrium Pb intragranular inclusions in copper had spherical shape at $T > 400$ °C, indicating isotropy of solid-liquid interface.

Thus, we can conclude that the isotropy of contact angle observed in our study at 450 °C is due to the isotropy of solid-liquid and solid-gas interfacial energy. This result is in contradiction with solid state wetting results, reported in Ref 10. Wynblatt at al. explains the observed effect by the anisotropy of interfacial energy on solid Pb-solid Cu interface. The authors (Ref 10) estimated the solid Pb/solid Cu interfacial energy as 926 mJ/m^2 for {100} and 1016 mJ/m^2 for {111} copper surface at 310 °C. This estimate does not agree with the data on intragranular Pb particle shape at 400 °C (Ref 26): {111} facettes were formed on the particle surface indicating that Pb/Cu {111} interface has a lowest energy among the other orientations. There are two possible explanations of this disagreement: (i) anisotropy of Pb/Cu interfacial energy is reversed on Pb solidification, energy of Cu {111}/Pb interface becomes higher than one of Cu {100}/Pb interface; (ii) contact angles measured in solid state wetting experiments are not the equilibrium ones.

6. Conclusions

On the basis of both experimental study and MD simulation of equilibrium contact angles and spreading kinetics of liquid Pb over polycrystalline and monocrystalline Cu substrates we can draw several conclusions

1. Anisotropy of contact angle is negligible above Pb fusion temperature due to practical isotropy of solid-gas and solid-liquid interfacial tensions.
2. Most of the data presented to date on the anisotropy of wetting and spreading for binary liquid metal/solid metal (or semiconductor) systems could be explained by selective oxidation of different substrate surfaces or by anisotropic dissolution of substrate in the melt. Contact angles obtained in the absence of dissolution on the sample surfaces free from impurities are isotropic (Ref 13).
3. Spreading of millimeter-size (Pb-Cu) drops over Cu substrate, which is not covered by the Pb monolayer, proceeds much slowly (10^2-10^3 s) comparing to other non-reactive liquid metal/solid metal systems such as Pb/Fe or Pb/W. This probably due to kinetic impediments for the triple line motion due to replacement of adsorbed on copper surface impurities by lead atoms. Equilibrium contact angle of Pb drop deposited on preliminary formed precursor film is reached within 10 ms, which is typical for non-reactive metallic couples.
4. Spreading anisotropy observed on the {110} Cu substrate could be attributed to strong anisotropy of precursor film development. If precursor film is preformed on {110} Cu surface, spreading anisotropy is vanished.

Acknowledgments

The authors are gratefully acknowledged Dr. S. I. Prokofjev and Prof. B.B. Straumal from ISSP RAS (Chernogolovka) for kindly supplied copper monocrystals. Financial support of Russian Foundation for Basic Research under Grant No. 11-08-01244-a is kindly acknowledged. The calculations were performed by using 'Chebyshev' SKIF MSU supercomputer.

References

1. Yu.Z. Povstenko, Anisotropy of Wetting and Spreading, *J. Math. Sci.*, 1993, **64**(3), p 890–898
2. D. Chatain, Anisotropy of Wetting, *Annu. Rev. Mater. Res.*, 2008, **38**, p 45–70
3. V.A. Presnov and A.P. Vyatkin, Wetting of Germanium by Indium and Solder Contacts of Semiconductors with Metals, *Surface Phenomena in Metals and Solders and Their Role in Processes of Powder Metallurgy*, Academy of Sciences of the Ukrainian SSR Press, Kiev, 1961, p 91–99 (in Russian)
4. A.P. Vyatkin and B.A. Selivanov, Production of Flat Alloyed Contacts with Germanium, *Izv. Visch. Ucheb. Zav. Fizika*, 1958, **5**, p 60–64 (in Russian)
5. R.W. Olesinski, N. Kanani, and G.J. Abbaschian, The Ge-In (Germanium-Indium) System, *Bull. Alloy Phase Diagrams*, 1985, **6**(6), p 536–539
6. N.F. Grigorenko, V.S. Zhuravlev, N.A. Krasovskaya, O.I.Tihomirova, V.V. Shishkov, Capillary Properties of an Indium-Tin Liquid Phase of Diffusion-Hardening Solders for a Germanium Solder, *Capillary and Adhesion Properties of Melts*, Naukova Dumka, Kiev, 1987, p 143–148 (in Russian)

7. B. Ressel, K.C. Prince, S. Heun, and Y. Homma, Wetting of Si Surfaces by Au–Si Liquid Alloys, *J. Appl. Phys.*, 2003, **93**(7), p 3886–3892
8. Z. Shi and P. Wynblatt, A Study of the Pb/Al(100) Interfacial Energy, *Metall. Mater. Trans.*, 2002, **A33**, p 2569–2572
9. Z. Shi, J.B. Lowekamp, and P. Wynblatt, Energy of the Pb{111} Parallel to Al{111} Interface, *Metall. Mater. Trans.*, 2002, **A33**, p 1003–1007
10. G. Rao, D.B. Zhang, and P. Wynblatt, A Determination of Interfacial Energy and Interfacial Composition in Cu-Pb and Cu-Pb-X Alloys by Solid-State Wetting Measurements, *Acta Metall.*, 1993, **41**, p 3331–3340
11. N. Eustathopoulos, M. Nicholas, and B. Drevet, *Wettability at High Temperatures*, Elsevier, Amsterdam, 1999, p 418
12. P. Protsenko, A. Terlain, and N. Eustathopoulos, Wetting of W by Liquid Pb and PbLi Alloys and Surface Interactions, *J. Nucl. Mater.*, 2007, **360**, p 265–271
13. P. Protsenko, J.-P. Garandet, R. Voytovych, and N. Eustathopoulos, Thermodynamics and Kinetics of Dissolutive Wetting of Si by Liquid Cu, *Acta Mater.*, 2010, **58**, p 6565–6574
14. S. Plimpton, Fast Parallel Algorithms for Short-Range Molecular Dynamics, *J. Comp. Phys.*, 1995, **117**, p 1–19
15. M.S. Daw, S.M. Foiles, and M.I. Baskes, The Embedded-Atom Method: A Review of Theory and Applications, *Mater. Sci. Rep.*, 1993, **9**, p 251–310
16. J.J. Hoyt, J.W. Garvin, E.B. Webb, III, and M. Asta, An Embedded Atom Method Interatomic Potential for the Cu–Pb System, *Model. Simul. Mater. Sci. Eng.*, 2003, **11**, p 287–300
17. H.S. Lim, C.K. Ong, and F. Ercolessi, Stability of Face-Centered Cubic and Icosahedral Lead Clusters, *Surf. Sci.*, 1992, **269**(270), p 1109–1115
18. S.M. Foiles, M.I. Baskes, and M.S. Daw, Embedded-Atom-Method Functions for the fcc Metals Cu, Ag, Au, Ni, Pd, Pt, and Their Alloys, *Phys. Rev. B*, 1986, **33**, p 7983–7991
19. D.R. Heine, G.S. Grest, and E.B. Webb, III, Surface Wetting of Liquid Nanodroplets: Droplet-Size Effects, *Phys. Rev. Lett.*, 2005, **95**(10), p 1–4
20. E.B. Webb, III, J.J. Hoyt, and G.S. Grest, High Temperature Wetting: Insights from Atomistic Simulations, *Curr. Opin. Solid State Mater. Sci.*, 2005, **9**(4–5), p 174–180
21. E.B. Webb, III, J.J. Hoyt, G.S. Grest, and D.R. Heine, Atomistic Simulations of Reactive Wetting in Metallic Systems, *J. Mater. Sci.*, 2005, **40**(9–10), p 2281–2286
22. E.B. Webb, III, G.S. Grest, and D.R. Heine, Precursor Film Controlled Wetting of Pb on Cu, *Phys. Rev. Lett.*, 2003, **91**(23), p 2361021–2361024
23. G.L.J. Bailey and H.C. Watkins, Surface Tension in the System Solid Copper-Molten Lead, *Proc. Phys. Soc.B*, 1950, **63**, p 350–358
24. C. Cohen, Y. Girard, P. Leroux-Hugon, A. L'Hoir, J. Moulin, and D. Schmaus, Surface Diffusion of Pb on (100) Cu: Coverage Dependence and Influence of Ordered-Phase Formation, *Europhys. Lett.*, 1993, **24**, p 767–772
25. D. Chatain, V. Ghetta, and P. Wynblatt, Equilibrium Shape of Copper Crystals Grown on Sapphire, *Interface Sci.*, 2004, **12**, p 7–18
26. L. Felberbaum, "Microstructure and Embrittlement of Leaded Copper Alloys," PhD Thesis, Lausanne, EPFL, 2005